AAS 95-110

SATELLITE DYNAMICS ABOUT EROS

D.J. Scheeres
Jet Propulsion Laboratory
California institute of Technology
Pasadena, California 91109-8099
email:dan_scheeres@zeus.jpl.nasa.gov

Abstract

The Near Earth Asteroid Rendezvous (NEAR) mission spacecraft will arrive at Asteroid 433 Eros in February, 1999. Following an initial period of characterizat Ion, the science phase of the mission will commence, and unprecedented information concerning an asteroid's shape, mass, density, composition and rotational dynamics will be sent to Earth for analysis. It will also mark the start of orbital operations about the most complex and irregular gravity field ever encountered in the history of space exploration. The severity of Eros' distortion from the usual spheroid bodies encountered in planetary exploration leads to fundamental differences in the orbital dynamics about it. Operations atrout Eros will also serve as an exciting test of orbit determination and prediction in an orbital environment which can be chaotic in some instances. This paper reviews the expected orbital dynamic environment of the NEAR spacecraft at Eros, discusses the problem of orbit control of the NEAR spacecraft 01 bitand presents the nominal mission plan.

The dynamical environment may be differentiated according to whether the spacecraft is close to or far from Eros. When far from Eros, the spacecraft must contend with the solar tide and solar radiation pressure (SRP) which arc large perturbations tc, the Eros attractive force. When close to Eros, the spacecraft must contend with the potentially irregular gravity field of the body- In this situation, there are potential orbits which are quite unstable and may crash onto the asteroid surface in a matter of days. Obviously, it is important to understand when and where such orbits exist, and how they may be avoided.

There arc a number of mission specific constraints which the NEAR spacecraft must operate under. These include both pointing, operational, and safety concerns as well as science directives and goals. The application of these constraints in the NEAR spacecraft environment at Eros is discussed, including some specific strategy implementations.

Combining the orbit control issues with the actual dates that the NEAR spacecraft arrives at Eros, a nominal plan is produced and briefly described which satisfies all the orbital constraints and fulfills specific science directives and goals. Some perturbations to this plan are briefly mentioned.

1 Introduction

The occasion of the first asteroid orbiter has forced thought to be given to the interesting problem of satellite dynamics about asteroids, specifically in the case of the NEAR mission of the dynamics of the NEAR spat.ec.raft about the asteroid Eros. The theory of asteroid orbiters shares some similarity with traditional theories of planetary orbiters, yet it is also much richer in many instances. Of specific interest are regimes of motion about an asteroid which are chaotic with a time scale on the order of days, allowing for such effects to be seriously considered and consciously avoided in deriving the control philosophy of the orbital phase. The existence of such dynamics was originally noted by J .1<.

Miller of the Jet I'repulsion Lab in the 80's, and has more recently been investigated in detail by Reference[Chauvineau et al.] and [Schemes].

In order to develop a robust and safe orbital plan for the NEAR mission, it is imperative that the genera] dynamics of such an orbiter be understood and that the orbit control be applied with the natural dynamics of the system in mind, so as to avoid dangerous or operationally intensive situations. The current paper gives a brief summary of the relevant dynamics which will be encountered by the NEAR spacecraft at Eros. It also reviews the current orbit control constraints and discusses bow they will be implemented during operations. Finally, it presents the nominal mission plan for orbital operations, as well as a description of this plan.

Section 2 lists the nominal parameters of interest for the NEAR spacecraft dynamics at Eros. For the spacecraft these include the spacecraft mass and total projected area. For the asteroid Eros, these include its orbital elements and its predicted size, density and rotational dynamics.

Section 3 discusses the dynamics the spacecraft will encounter when further than ~200 km from Eros. For such a small central body, the solar tide and solar radiation pressure become significant effects which must be properly understood and modeled. Topics of discussion include long term stability of the NEAR spacecraft in a far orbit and a direct comparison of the different perturbations acting on the spacecraft orbit. Section 4 discusses the dynamics the spacecraft will encounter when close to Eros. Included is a discussion on periodic orbits, orbits stable against crashing on the asteroid, resonance effects and some general results on retrograde orbiters. The complicated nature of the dynamics in some orbital regimes is highlighted, and attempts are made to map out regions where the NEAR spacecraft can orbit in relative safety.

Section 5 lists the heuristic mission constraints for the NEAR orbits] mission and proceeds to detail how each will be met. The control problem can be decomposed into control of the asteroid inclination, node and radius. Specific methodologies to be used are discussed. Some of tbc details of timing control arc briefly mentioned as well. Section 6 presents the current nominal mission p]an which adheres to the stated mission constraints and satisfies the nominal science requirements.

2 Spacecraft and Asteroid Definition

As this paper deals with a specific mission, with a well defined spacecraft and a fairly well defined asteroid, it is possible to inject real numbers and parameters into tile discussion.

2.1 NEAR Spacecraft Parameters

At launch the NEAR spacecraft will weigh in at approximately 805 kg. During the inter-planetary cruise and Eros rendezvous, the craft will usc the major portion of its fuel and its mass at the start of orbital operations will be approximately 500 kg. The total area of the NEAR spacecraft solar arrays are 9 m^2 and are mounted on a bus of approximate area 3.24 m^2. This leads to an estimate of the total spacecraft area subject to solar radiation pressure (SRP) of 12.24 m^2. A parameter of interest is the spacecraft mass to area ratio, designated as B. For the NEAR spacecraft after Eros rendezvous, this parameter will have a value of $B \approx 40.85$ kg/m^2. This parameter drives the effect which the SRP has on the spacecraft orbits.

2.2 Eros Parameters

The orbital parameters of Eros have been determined by Yeomans as (REF[Yeomans]):

$$a = 1.4583 \text{ AU} \quad (1)$$

$$e = 0.2230 \quad (2)$$

$$i = 10.8308 \text{ deg} \quad (3)$$

$$\omega = 178.5677 \text{ deg} \quad (4)$$

$$\Omega = 304.4405 \text{ deg} \quad (5)$$

$$T_o = 1996 \text{ March } 12.S183 \quad (6)$$

Some additional parameters of the orbit are the orbital period, $T_P = 1.76$ years, and the radius of perihelion and aphelion, 1.1331 and 1.7835 AU respectively. Finally, the angular rate of Eros about the sun, N', will vary from 1.8255×10^{-7} rad/s at perihelion to 7.3685×10^{-8} rad/s at aphelion.

The actual size, shape, density and rotational dynamics of Eros are currently unknown, although there arc bounds and estimates on all of these parameters. Reference [Yeomans] gives a shape bound on Eros of $40.5 \pm 3.1 \times 14.5 \pm 2.3 \times 14.1 \pm 2.3$ km, and a spin period of 5.27011 hours with its rotation pole located at an ecliptic latitude and longitude of 11° and 16° respectively (B1950, uncertain by a few degrees). These nominal numbers are used throughout this paper, except where noted (in the section on periodic orbit families and zero-velocity curves), As Eros is classified as an S type asteroid, a reasonable supposition for its density is 3.5 g/cm^3, although this value is quite uncertain. Given these, all that is needed to finally specify the Eros model is a shape. A tri-axial ellipsoid model is assumed for most computations with the nominal size as given by Yeomans. For the computation of the zero-velocity surfaces, periodic orbits and equilibrium points, the APL-0 shape model for Eros is used. This shape model is briefly described in Section 4. Once the actual Eros parameters are determined, they will be substituted into the analysis.

Based on the expected values of Eros size and density, the gravitational parameter used in this paper is:

$$\mu = 1.012 \times 10^{3} \text{ km}^3/\text{s}^2 \quad (7)$$

The most important terms of the harmonic expansion of the gravity field correspond to the second degree harmonics, C_{20} and 6'22. For the tri-axial ellipsoid J ros model these are:

$$C_{20} = -36.3/r_o^2 \quad (8)$$

$$C_{22} = 17.9/1,: \quad (9)$$

where r_o is an arbitrary normalization radius

3 Spacecraft Dynamics Far From Eros

When sufficiently far from Eros (> 200 km), it is acceptable to approximate the asteroid as a point mass (for modeling the gross properties of the dynamics). Note that some of the lower degree gravity harmonics may be detectable at these distances, but they have no major affect on the trajectory. For studying this case, choose preference frame centered at Eros and rotating so that the $-X$ axis always points at the sun. Choose the Z axis along the angular momentum vector of Eros' orbit about the sun, and then choose the Y axis according to tile right-hand rule.

In this regime, the significant forces arise from the attraction of Eros, tile tidal force of the sun and the solar radiation pressure (SRP) acting on the spacecraft. Assuming that the spacecraft solar arrays are oriented to face the sun the equations of motion can be stated as:

$$\ddot{X} - 2N'\dot{Y} = -\frac{\mu X}{R^3} + 3N'^2 X + g \quad (10)$$

$$\ddot{Y} + 2N'\dot{X} = -\frac{\mu Y}{R^3} \quad (11)$$

$$\ddot{Z} = -\frac{\mu Z}{R^3} - N'^2 Z \quad (12)$$

where g is the SRP force delivered to the spacecraft, N' is the angular rate of Eros about the sun and R is the radius of the spacecraft from the center of Eros. The SRP acceleration is computed to be (REF[Scheeres]):

$$g = 1.0880 \times 10^{-10} \frac{1}{R^2} \text{ km/s}^2 \quad (13)$$

where $\mathcal{R}$ is the radius of Eros' orbit about the sun in AU. For the NEAR spacecraft at Eros this parameter will range from $8.47 \times 10^{-}$" km/s^2 at perihelion to 3.42×10^{-11} km/s^2 at aphelion.

3.1 Stationary Points

Of interest for this dynamical system are those points where a spacecraft would ideally remain at rest if placed there with no relative velocity. In the absence of SRP forces, the tidal and Eros attraction' forces will cancel out at the locations:

$$X_E = \pm \left(\frac{\mu}{3N'^2}\right)^{1/3} \tag{14}$$

$$\approx \pm 2163.494 \rightarrow *3961.177 \text{ km} \tag{15}$$

where the range depends on whether Eros is at perihelion or aphelion.

The addition of SRP forces modifies the location of these stationary points. The equation from which to solve for them becomes:

$$\left(\frac{X}{X_E}\right)^3 + \epsilon \left(\frac{X}{X_E}\right)^2 - \frac{X}{|X|} = 0 \tag{16}$$

$$\epsilon = \frac{g}{3N'^2 X_E} \tag{17}$$

At perihelion the parameter $\epsilon = 0.3916$, while at aphelion the parameter is $\epsilon = 0.5301$. Analytically, the location of these new points arc:

$$X_S = \pm X_E \left[1 \mp \frac{1}{3}\epsilon + \frac{1}{9}\epsilon^2 + \cdots\right] \tag{1s}$$

which is accurate to the order of 10 kilometers. Solving the equations exactly yields the following stationary points for the Eros-NEAR spacecraft system:

$$X_S = \begin{cases} 1915, & -2486 \text{ km at perihelion} \\ 3371, & -4799 \text{ km at aphelion} \end{cases} \tag{19}$$

These stationary points are, of course, unstable and would require some sort of closed loop control for the spacecraft to remain in their vicinity. From a mission poiut of view these solutions are not necessarily interesting either. They are useful in that they characterize where the solar tide, gravitational and SRP forces are equal, and hence delineate where the Eros gravity field begins to dominate.

3.2 Stability of Spacecraft Orbits

A question of interest is whether or not a spacecraft is bound to an asteroid for a long time duration, or if the spacecraft might escape over a fairly short time if not controlled. These questions may be answered by a quick study of the zero-velocity curves of the current system.

First note that Equat ions 10- 12 have a Jacobi integr al, stated as:

$$C_s = \frac{\mu}{R} + \frac{3}{2}N'^2X^2 - \frac{1}{2}N'^2Z^2 + gX - T \tag{20}$$

where C_s is the Jacobi constant and T is the kinetic energy of the spacecraft with respect to the current coordinate frame. In actuality the angular rate N' varies in time and thus the integral does not truly exist. However, over short periods of time it is useful to approximate the time varying N' with a constant value.

The zero-velocity curves are found by equating the kinetic energy T to zero and solving the resultant equation. See Figure 1 for a projection of the zero velocity surface into the X-Y plane for

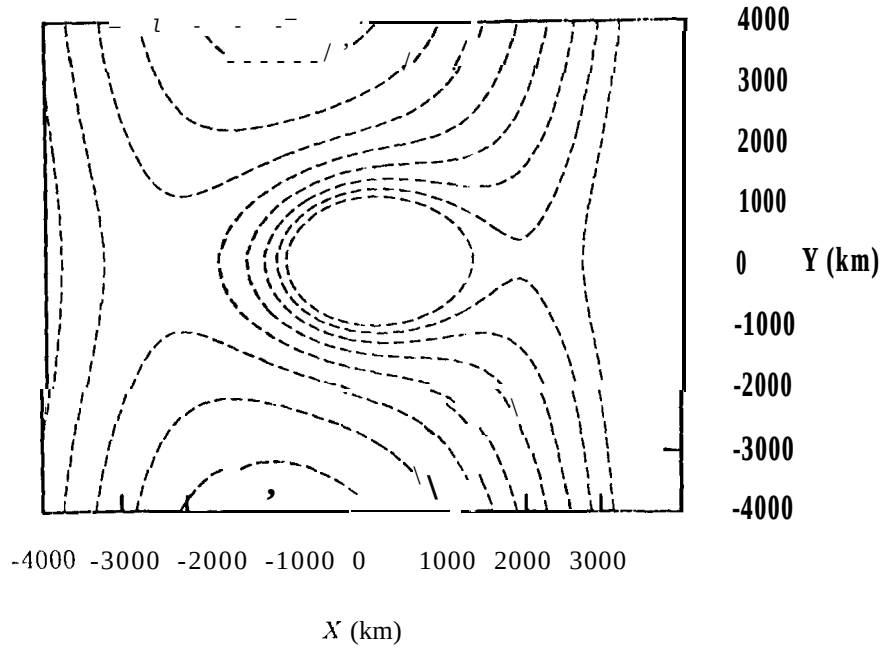

Figure 1: Zero-Velocity Curves in the X-Y Plane

the current case at periapsis. The location of the two stationary orbits can be clearly seen in this figure.

Given a spacecraft initially close to the asteroid, a criterion for it to remain close to the asteroid and not escape is that its Jacobi constant have a value $C_s > C_4$, where C_4 is the Jacobi constant of the 4th stationary point along the $+X$ axis, When this inequality is satisfied, the spacecraft cannot leave the vicinity of the asteroid ancl escape; when it is not satisfied, the possibility exists, At the stationary points the Jacobi constant can be approximated by:

$$C_{\pm} = \frac{5}{2}N'^2X_E^2 \pm gX_E + \cdot \tag{21}$$

For the NEAR-Eros system the value of this constant, C_4 ranges from 5.73 x 10^{-7} km^2/s^2 at perihelion to 3.48x 10^{-7} km^2/s^2 at aphelion.

At Eros rendezvous, the NEAR spacecraft will initially orbit Eros in a circular orbit close to the terminator (i.e. close to the solar plane-of-sky). Thus it is of interest to apply the capture criterion to such an orbit. Assume a circular orbit with its orbit angular momentum pointed towards the sun. Then the Jacobi integral can be written as:

$$C_s = \frac{1}{2}\left[\frac{\mu}{a} - a^2N'^2\right] \tag{22}$$

Applying the stability criterion yields the inequality:

$$a^3 + \frac{2C_{\pm}}{N'^2}a - \frac{p}{N'^2} < 0 \tag{23}$$

It is easy to see that there is a unique positive value of a below which the inequality is satisfied. For our situation, this value ranges from 865 km at periapsis to 1432 km at apoapsis. Note that the initial NEAR orbit is circular at 1000 km with Eros approaching perihelion, indicating that if

left unattended for a sufficient period of time, the spacecraft may escape from the vicinity of Eros. Nominal mission plans only call for the spacecraft to be at this radius for a period of a few weeks while the time scale for unstable behavior is on the order of hundreds of days, making this type of instability controllable and not an issue. Of greater concern is that the eccentricity of this initially circular orbit approaches 1 after approximately 140 days (see Reference [Scheeres]), placing a finite time on how long such an orbit could be left unattended. Note that an orbit in the solar plane-of-sky with a semi-major axis of 1000 km, an eccentricity of 0.794 (206 x 1794 km) and a properly chosen argument of periapsis will remain trapped at Eros in the solar plane-of-sky for an arbitrarily long period of time (see Reference [Scheeres]). All following orbits will be at radii of 200 km or less and hence for the remainder of the mission the NEAR spacecraft will be definitely trapped at Eros.

3.3 Comparison With Gravity Harmonics Effects

Of interest is the effective sphere of influence of the various perturbations acting on the spacecraft, the main ones being the solar tide, solar radiation pressure and the gravity harmonics of Eros. An efficient way in which to measure these effects is to compare how these different forces affect the spacecraft orbit, notably how they effect the secular rate of change in the orbit node and periapsis. In general, far from Eros the tidal force will dominate, while at intermediate distances the SRP force dominates and at close distances the gravitational harmonics dominate.

In REF [Scheeres] some explicit formulae which compare these effects are given. To make the proper comparison the following constants must be computed and compared:

$$\begin{aligned} C_t &= \frac{3N'^2}{4\sqrt{\mu}}\, a^{3/2} \quad \text{Scalar Tide Effect} \\ C_g &= \frac{3g}{2\sqrt{\mu}}\sqrt{a} \quad \text{SRP Effect} \\ C_j &= \frac{3\sqrt{\mu}J_2 r_o^2}{2a^{7/2}} \quad \text{Gravity Harmonics Effect} \end{aligned} \tag{24}$$

where each of these coefficients measures the potential secular rate of the node and argument of periapsis. Of interest are the ratios of C_t/C_g and C_g/C_j which compare the solar tide to the SRP and the SRP to the harmonics, respectively. Evaluating these ratios at Eros perihelion yields:

$$C_t/C_g = \frac{N'^2 a}{2g} \tag{25}$$

$$= 1.97 \text{ x } 10^{-4} a$$

$$C_g/C_j = \frac{g a^4}{\mu J_2 r_o^2} \tag{26}$$

$$= 3.48 \text{ x } 10^{-9} a^4$$

Equating the ratios to 1, we find that the SRP has a dominant effect Over the solar tide **for** $a < 5084$ km, and that the gravity harmonics has a dominant effect over the SRP for $a < 144$ km. Note that there is a relatively long period of time when the spacecraft orbit radius is at 200 and 1000 km, implying that the SRP effect on its orbit will be the largest perturbation during this time.

4 Spacecraft Dynamics Close to Ems

Given a gravitational field and the rotational state of the model, the equations of motion of the spacecraft may be written down. The most efficient expression of these equations is given in the body-fixed frame of the asteroid. Given an integrated result in this frame, it is fairly easy to transform back to the inertial frame. The benefit of this formulation is that no rotational transformations must be made to evaluate the accelerations due to Eros' gravity.

Allowing for a genera] determination of the rotational dynamics, the body fixed equations of motion for a small particle are (Greenwood, 1965, pp 50-51):

$$\ddot{\mathbf{r}} + 2\Omega \times \dot{\mathbf{r}} + \Omega \times (\Omega \times \mathbf{r}) + \dot{\Omega} \times \mathbf{r} = U_{\mathbf{r}} \tag{27}$$

where $\mathbf{r}$ is the body-fixed vector from the asteroid center of mass, (--) and (-- ¨) are first and second time derivatives with respect to the body-fixed, rotating frame, Ω is the instantaneous rotation vector of the body with respect to inertial space and has magnitude $|\Omega| = \omega$, and $U_{\mathbf{r}}$ is the gradient of the gravitational potential.

Note that this formulation allows for a non-constant rotation rate of Eros. Should there be a non-principal axis rotation state, the tenor of the dynamics will be quite different in some instances. First of al], since the asteroid will be following the dynan lies of a torque-free rigid body rotation state, the angular velocity vector Ω in the body fixed frame will be periodic, and hence the equations of motion will be time-periodic. Other consequences are that the Jacobi integral will not exist, and neither will the classical stationary orbits (they transform into periodic orbits). There are also a number of other important consequences, some of which tend to stabilize the dynamics and some of which tend to de-stabilize tile dynamics, but these are not discussed here.

It is expected that Eros will be in near principal axis rotation, thus we assume that $|\dot{\Omega}| \equiv 0$ and $|\Omega| = w = 3.3118 \times 10^{-4}$ radians/second (corresponding to a rot at ion period of 5.27 hours). Equate the direction of rotation with the z-axis and fix the x-axis along the smallest moment of inertia; tile definition of the y-axis follows by the right-hand rule. The equations of motion in scalar form are then:

$$\ddot{x} - 2\omega\dot{y} = \omega^2 x + U_x \tag{28}$$

$$\ddot{y} + 2\omega\dot{x} = \omega^2 y + U_y \tag{29}$$

$$\ddot{z} = U_z \tag{30}$$

4.1 Jacobi Integral

Note that due to the assumption of a uniform rotation rate a Jacobi integral exists for this problem, independent of the degree of irregularity of the gravitational field. To establish the integral's existence one need only note that the equations of motion in the uniformly rotating, body-fixed frame are time-invariant. The Jacobi constant C is defined by the relation:

$$C = V(x, y, z) - T \tag{31}$$

where

$$V(x, y, z) = \frac{1}{2}\omega^2(x^2 + y^2) + U(x, y, z) \tag{32}$$

is the modified potential and

$$T = \frac{1}{2}(\dot{x}^2 + \dot{y}^2 + \dot{z}^2) \tag{33}$$

is the kinetic energy of the particle with respect to the rotating asteroid. Given any initial conditions, the constant C is conserved for the ensuing motion.

4.1.1 Zero-Velocity Curves

The z~.ro-velocity surfaces are defined for this system by the equation:

$$V(x, y, z) = C \tag{34}$$

which defines a 2-dimensional surface in the 3-dimensional $x - y - z$ space. Following is a section of the mro-velocity surface taken along the z =- O plane using the APL-0 model (a hypothetical model of Eros' shape specified hy 4202 vertices and 8400 triangular faces). Note the lack of symmetry, which will be expected in the real asteroid shape as well.

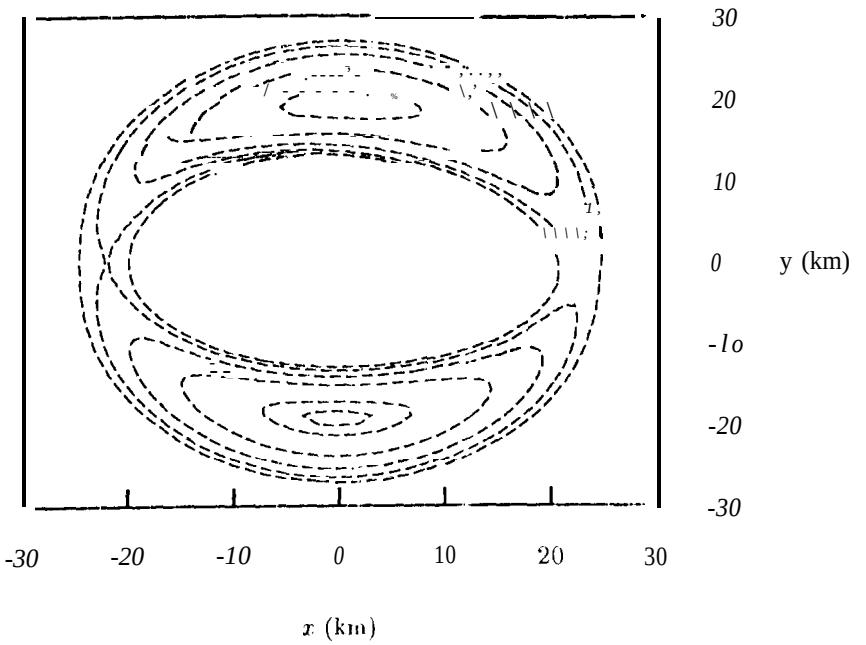

Figure 2: Zero-Velocity Curve in the x - y (z = O) Plane

Note the four areas where the zero-velocity curves intersect or close in upon themselves. Located here are equilibrium points, which are discussed in further detail in Section 4.2.

4.1.2 Stability Against Crashing

The zero- velocity curve analysis can provide a ready estimate of when the spacecraft is not in danger of crashing onto the asteroid surface. The criterion was initially derived in REF[Scheeres] for an attracting ellipsoid shape, but can easily be extended to a general gravitational potential. It is developed as follows. Define the equilibrium point along the $\pm x$ axis as the $\pm S$(addle) equilibrium points, It is seen that these are the first points to bifurcate as the Jacobi constant decreases from large, positive values. For any orbiter with a Jacobi constant $C > C_{\pm S}$, the orbit is then separated from the asteroid by the zero- velocity surface, which it cannot cross. Thus, in these situations the spacecraft is definitely stable against crashing on the asteroid, although it may still be ejected from the asteroid on a hyperbolic orbit. Figure 3 presents a curve which delineates between those orbits which are definitely stable against crashing on the asteroid and those which are not. This curve only applies to orbiters with an inclination within $\sim 10°$ of the equator.

Note that this criterion only applies to direct, near-equatorial orbits. For retrograde, near-equatorial orbits the results from Section 4.3 apply instead, and establish a uniform stability against crashing. Currently, there is no uniformly applicable criterion for the case of near-polar orbits,

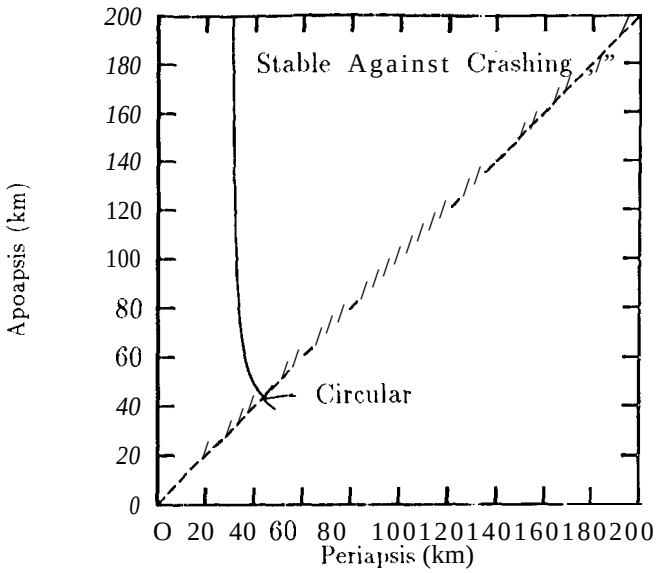

Figure 3: Curve for stability against crashing for low inclination orbiters

4.1.3 Resonance Effects

A simple, and illustrative, result can be derived which estimates the expected change in 2-body energy due to spacecraft interaction with the 2nd order gravitational harmonics. To begin the characterization, express the 2-body energy in terms of body-fixed coordinates and tile Jacobi integral. Doing so yields:

$$C_2 = \sum_i U_i + (\Omega \times \mathbf{r}) \cdot (\Omega \times \mathbf{r}) + \Omega \cdot (\mathbf{r} \times \dot{\mathbf{r}}) - C \tag{35}$$

where the gravitational potential U has been expressed as $U = p/r + \sum_i U_i$, where the $[J_i$ represent the higher orders of the gravitational potential. Differentiating the expression with respect to time yields:

$$\dot{C}_2 = \sum_i \nabla U_i \cdot \dot{\mathbf{r}} + 2\,(\Omega \times \mathbf{r}) \cdot (\Omega \times \dot{\mathbf{r}}) + \Omega \cdot (\mathbf{r} \times \ddot{\mathbf{r}}) \tag{36}$$

Substitute for $\ddot{\mathbf{r}}$ from the equations of motion and simplify t o find the final result:

$$\dot{C}_2 = \sum_i \nabla U_i \cdot (\dot{\mathbf{r}} + \Omega \times \mathbf{r}) \tag{37}$$

$$= \sum_i \nabla U_i \cdot \dot{\mathbf{r}}_I \tag{38}$$

where $\dot{\mathbf{r}}_I$ is the spacecraft velocity vector as evaluated in inertial space. Note that the gravitational potentials U_i are still evaluated in the body-fixed, non-inertial coordinate system. This may also be related to the time derivative of the osculating semi-major axis, as:

$$C_2 = -\frac{\mu}{2a} \tag{39}$$

$$\dot{C}_2 = \frac{\mu}{2a^2}\dot{a} \tag{40}$$

By comparison to the standard equations for the time derivatives of the osculating elements (REF[Kaula]) we note the interesting relationship:

$$n\frac{\partial F}{\partial M} = \sum_i \nabla U_i \cdot \dot{\mathbf{r}}_I \tag{41}$$

where n is the mean motion, F is the perturbing potential and M is the mean anomaly.

in the following discussion! we only consider the gravity potential of 2nd degree:

$$U_2 = \frac{\mu}{r^3}\left[\frac{r_o^2 C_{20}}{2}\left(3\sin^2\alpha - 1\right) + 3r_o^2 C_{22}\left(1-\sin^2\alpha\right)\cos(2\lambda)\right] \tag{42}$$

The gradient of this yields:

$$\nabla U = \left(U_r - \frac{\sin\alpha}{r}U_{\sin\alpha}\right)\hat{\mathbf{r}} + \frac{U_\lambda}{r\cos^2\alpha}\left(\mathbf{k}\times\hat{\mathbf{r}}\right) + \frac{1}{r}U_{\sin\alpha}\mathbf{k} \tag{43}$$

where the angle λ is the longitude of the spacecraft in the body-fixed coordinate system.

In the following, we apply this formula to the case of a direct, equatorial elliptic orbit and derive an estimate on the total variation one may expect in the energy and semi-major axis from one periapsis passage. Assuming that the orbital motion takes place in the equatorial plane, we have sin α = O and cos α = 1. Next, assume that we evaluate the equation in the vicinity of periapsis, and that periapsis remains constant during one passage, Performing a quadrature of these equations symmetrically around periapsis eliminates any terms which are odd about periapsis and yields (approximately):

$$\Delta C_2 \approx -\frac{6\mu r_o^2 C_{22}}{r_p^4}\sqrt{\frac{\mu r_a}{2r_p(r_a+r_p)}}\sin 2\nu\left[\frac{(1-r_p/r_a)}{|2\omega/3 - \dot{f}_p|} + \frac{4}{|\omega - \dot{f}_p|}\right] \tag{44}$$

where

$$\dot{f}_p = \sqrt{\frac{\mu(1+e)}{r_p^3}} \tag{45}$$

is the angular rate of the spacecraft at periapsis. This relation only approximate and indicates the largest transient variation which may be seen in C_2, not necessarily the total variation in one pass.

Several conclusions can be immediately drawn from these relationships. First, if the argument of periapsis lies in the 1st or 3rd quadrant of Eros, the energy of the orbit will suffer a net decrease and draw apoapsis towards the asteroid. Conversely, if the argument of periapsis lies in the 2nd or 4th quadrant, the energy will suffer a net increase, and rosy catapult tile spacecraft into an escape trajectory. Consider a brief example. Suppose a spacecraft is in an elliptic orbit with r_a = 90 km and r_p = 40 km. Assuming that the orbit is direct and equatorial the change in apoapsis and periapsis is estimated to be:

$$\Delta r_a \approx -19\sin 2\nu \text{ km} \tag{46}$$

$$\Delta r_p \approx 2\sin 2\nu \text{ km} \tag{47}$$

Such a large variation in the apses from orbit to orbit is not acceptable.

Figure 4 plots the radius, periapsis and apoapsis of a spacecraft in a direct, equatorial orbit with a periapsis passage through the 1st quadrant of Eros. Figure 5 plots the same situation except with a periapsis passage through the 2nd quadrant of Eros. Note how the apoapsis changes as expected. Both results are from a precision trajectory integration.

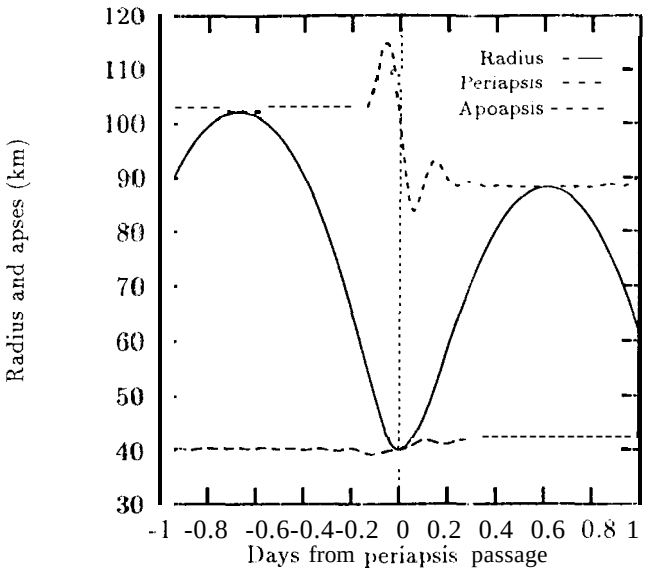

Figure 4: Radius, Periapsis and Apoapsis for a 1st Quadrant Flyby

4.2 Body-Fixed **Periodic** Orbits

In a non-integrable environment such as Eros', it is difficult to come up with definitive conclusions on general spacecraft motions. Exceptions to this arise when either far from the asteroid or in near-equatorial, retrograde orbits about the asteroid. When not in these conditions, recourse must be made to other approaches to build up a picture of the dynamics about the asteroid. The computation and analysis of body-fixed periodic orbits is the first, and simplest, step towards understanding these complicated dynamics. The main intent is to determine tile stability of these orbits, as this then provides information which impacts the stability and predictability of orbits in the region of these families.

Clear from Figure 2 is the existence of four equilibrium points about the A PL-0 Eros model. At these points there will be a net zero acceleration acting on the particle in the rotating frame. These are circular orbits which are exactly synchronous with Eros' rotat ion rate. A more direct manner of computing these orbits, or equilibrium points, *is by* solving the algebraic equations:

$$V_x(x,\ y, z) = o \tag{48}$$

$$V_y(x,\ y, z) = o \tag{49}$$

$$V_z(x,\ y, z) = o \tag{50}$$

for all values of x, y, z which satisfy them. Note that there is no *a priori* number of solutions to these equations. Depending on the shape and spin rate of the body, there could be a different number of solutions. It is important to note that these solutions exist uniquely despite the lack of symmetry in the gravity field.

For the nominal Eros model all four of the synchronous orbits arc unstable. The two points located near the ends of the asteroid are hyperbolically unstable, thus any particle displaced from these body-fixed points will depart from that point on a local hyperbola. The two points located along the long side of the asteroid are complex unstable, thus any particle displaced from these orbits will depart from that point on a local spiral. As all the synchronous orbits about Eros are unstable (for all current models), it may be classified as a Type 11 asteroid (REF[Scheeres]).

A number of periodic orbit families have been found for the current h-es models. These arc conveniently split into three main groups (not counting the equilibrium points): direct, near-equatorial orbits; retrograde, near-equatorial orbits; near-resonant, non-planar orbits.

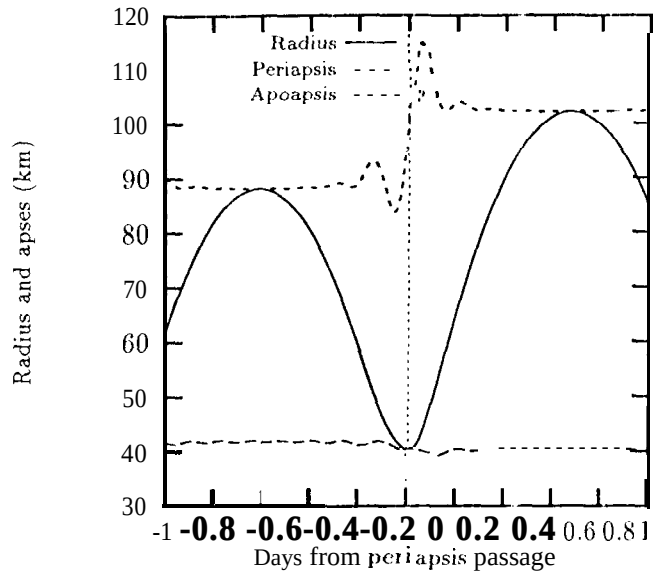

Figure 5: Radius, Periapsis and Apoapsis for a 2nd Quadrant Flyby

The direct, near-equatorial family originates as a circular, equatorial family far from the asteroid, As it moves to smaller radii, it retains this character until it bifurcates into two elliptical orbit branches. These families are stable until they reach a radius of approximately 37 km, where they become unstable (Reference [Scheeres]). The instability of these orbits is rather severe, as the unstable manifolds tend to interact closely with the asteroid surface and cause a perturbed particle to impact, or escape from the asteroid in a short time scale on the order of days or weeks, In general, any direct orbit with a periapsis less than 40 to 50 km should be carefully investigated to ensure that it does not suffer large changes to its osculating elements.

The retrograde, near-equatorial family also originates as a circular, equatorial family far from the asteroid. However, as it moves to smaller radii, it never bifurcates in the plane and retains its circular character until it terminates by intersection with the asteroid surface. This family remains stable up to intersection with the asteroid surface, indicating that it is an attractive candidate for flying close to the asteroid surface.

The near-resonant, non-planar orbits tend to exist only in the vicinity of select radii where the particle's period of out-of-plane oscillation is commensurate with the asteroid rotation rate. When this situation occurs, it is possible for the particle orbit to close upon itself in the body-fixed reference frame. This, in turn, allows for an analysis of the stability of this motion. Otherwise, it is difficult to ascertain the stability of such non-planar orbits. Two main families of these orbits have been found. One of these families emanates from the halo orbits surrounding the equilibrium points discussed previously and travel through polar orbits and terminate on another of the equilibrium points' halo orbit. Such families remain unstable throughout, and have a radius of approximately 20 km. A second pair of such non-planar families has a period roughly twice the rotation period of Eros at a radius of 30 to 35 km. This family remains unstable throughout most of its evolution as well, except for a small portion when it retains much of its near- circular character and its inclination grows above $\approx 130°$. 'he existence of this stable interval is important as it provides an indication of the degree to which a retrograde, near-circular orbit may depart from the equator and still retain its stability. in this instance, it appears that orbit inclinations less than 130° at an orbit radius of $\sim$35 km are definitely unstable.

4.3 Non-Synchronous Motions

When in an orbit far from the asteroid or in a retrograde, near-equatorial orbit, there is a simplification which can be introduced into the problem. In both of these conditions (as discussed in REF[Scheeres]), the gravitational potential U may be replaced by a rotationally symmetric potential without compromising the nature of the dynamics. This simplifies the analysis a great deal, as then one may refer to the theory of planetary orbiters for which there is a wealth of literature (Reference [...]).

In such an environment, it is fruitful to describe the orbits in terms of averaged osculating elements, as these contain most of the information and dynamics of interest. Then it is well established that the semi-major axis, eccentricity and inclination remain constant on average with short period oscillations. The remaining elements; the argument of periapsis, the longitude of the ascending node and the epoch of periapsis, contain secular variations. Retaining only the lowest degree gravitational parameter $C_{20} = -J_2$, the dynamics of these elements are described by (REF[Danby]):

$$\frac{d\Omega}{dt} = -C_j \cos i \tag{51}$$

$$\frac{d\omega}{dt} = -C_j \left[\frac{5}{2}\sin^2 i - 2\right] \tag{52}$$

$$\frac{dM_o}{dt} = n - C_j \sqrt{1-e^2}\left[\frac{3}{2}\sin^2 i - 1\right] \tag{53}$$

where

$$C_j = \frac{3n J_2 r_0^2}{2p^2} \tag{54}$$

$$n = \sqrt{\frac{\mu}{a^3}} \tag{55}$$

$$p = a(1-e^2) \tag{56}$$

For the nominal Eros model at an orbital radius of 35 km (and in a retrograde orbit), the value of C_j is 33.8 degrees/day, at an orbital radius of 50 km the value of C_j is 9.7 deg/day. Thus, when within a few radii of Eros, the secular change in the node and argument of periapsis may be quite large.

5 Orbit Control

The orbit control philosophy on the NEAR spacecraft may be broken into two phases. The first phase deals with orbits that have periapsis greater than 100 km. in this regime traditional targeting approaches can be used, and these should suffice to control the orbit to the desired level of accuracy. The second phase concerns itself with orbits that have their periapsis within 100 km of the asteroid. in this regime, special care must often be taken in designing a control methodology and in targeting the spacecraft maneuvers to achieve specific spacecraft states. The following section deals exclusively with the control of orbits when within 100 km of the asteroid.

5.1 Mission Constraints

Once the spacecraft achieves orbit about Eros and the science phase of the mission begins, there are a number of mission design constraints which must be adhered to. These constraints drive the control of the orbit during this phase and place restrictions on what orbits are flown and when they arc flown. A heuristic statement of the mission design constraints follow:

- The spacecraft orbit should be safe and stable for a t imespan of weeks

- The spacecraft orbit normal should lie within 30° of the Earth when in low orbits (e.g. 35 km radius), and lie within 20° of the Earth when in high orbits (e.g. 50 km radius and higher)
- The spacecraft orbit normal should lie within 20° of the Sun for the first 100 days of the science phase mission, and lie within 300 of the Sun for the remainder of the mission
- Normally, there shall he no less than 7 clays between maneuvers
- The total orbital mission phase AV expenditure shall remain less than 100 m/s
- The spacecraft shall orbit as low as possible (nominally at a 35 km radius) for as long as possible without violating *any* of the above constraints

The two constraints on the spacecraft orbit normal are actually to be applied to the spacecraft orientation itself. However, assuming a nominally nadir pointing spacecraft, these constraints may be applied to the orbit normal. These mission design constraints can be realized by controlling the spacecraft orbit inclination, node and radius. These are discussed in more detail below.

5.2 Inclination Control

The first constraint on the orbit is that it be safe and stable during the mission duration. This constraint is most easily met by specifying that the orbit must always be retrograde with respect to the asteroid rotation pole. Flying the orbit in this mode will usually ensure that the spacecraft will be non-synchronous with the asteroid rotation rate and not affected by the instabilities associated with direct orhits. To keep this constraint throughout the mission will require that the spacecraft orhit be changed by 180° around the mid-point of the mission (at a nominal cost of 8.3 m/s). This is necessary since the rotation pole of Eros lies in its orbital plane and since the orbit normal must follow the Sun and Earth. Note that when the spacecraft is in an especially close orbit, such as the 35 km orbits, the inclination restriction must be tight ened. nom analysis involving periodic orbit families, it is seen that this constraint is $i > 130°$ at least. At 50 km orbits, the constraint can be relaxed to $i \geq$ '30°.

Following this retrograde strategy should also ensure that the inclinat ion, semi-major axis and eccentricity will suffer no long-term secular effects, although they may have sizable short period oscillations.

5.3 Plane-of-Sky Control

Forcing the orbit plane to comply with the two plane-of-sky constraints consumes the majority of effort during the orbital phase, and drives the mission profile for the most part. A plane-of-sky constraint angle of i_C forces the orbit normal to point within i_C degrees of the body in question (the Earth or Sun). Under the natural dynamics of the orbit plane about the asteroid, the orbit normal will precess shout the asteroid rotation pole and usually will leave the constraint cone after a while. Prior to this violation a plane change maneuver must be performed to reset the orbit normal within the constraint cone again. Ideally, the plane change maneuver will not change the orbit inclination, but will only rotate the argument of the ascending node, as measured in the asteroid equator.

Often, in planetary situations, a plane change maneuver is executed so as to minimize fuel consumption. This is usually possible by raising apoapsis to a higher altitude and effecting the change there, where the fuel cost is less. In the NEAR mission application such a fuel optimal scheme is not followed for several reasons, the foremost being that the total fuel cost for making a plane change maneuver is fairly small due to the small speeds of the spacecraft about the asteroid, and that such an implementation would waste precious time and make the orbit operations phase more intense. Rather, in designing the orbit plane control it is the maneuver frequency which is minimized (i.e., the time between maneuvers is maximized) This is effected by understanding the orbit plane dynamics and reseting them so that the time to the next constraint violation is maximized. This approach is briefly discussed in the following, for both one and two constraints.

5.3.1 Single Constraint

First define the orbit normal vector and the constraint vector:

$$\mathbf{u}_h = \sin\Omega \sin i\hat{x} - \cos\Omega \sin i\hat{y} + \cos i\hat{z} \quad (57)$$

$$\mathbf{u}_1 = \sin\Omega_1 \sin i_1\hat{x} - \cos\Omega_1 \sin i_1\hat{y} + \cos i_1\hat{z} \quad (58)$$

where $\hat{x}, \hat{y}$ and $\hat{z}$ are the unit vectors associated with an equatorial, inertial coordinate system chosen so that the asteroid rotation pole lies along the $\hat{z}$ direction and the equator lies in the $\hat{x}$-$\hat{y}$ plane, Ω is the orbit node, i is the orbit inclination, Ω_1 is the node of the constraint vector and i_1 is the inclination of the constraint vector. Associated with the constraint vector is a constraint angle i_{C_1} which we currently assume to be $< \pi/4$. The plane-of-sky constraint then states that the orbit normal vector must lie within an angle i_{C_1} of the constraint vector $\mathbf{u}_1$, defining a cone about the vector $\mathbf{u}_1$. The plane-of-sky inclination of the spacecraft orbit is the angle P, defined as $\cos P = \mathbf{u}_h \cdot \mathbf{u}_1$, or explicitly as:

$$\cos P_1 = \sin i \sin i_1 \cos(\Omega_1 - \Omega) + \cos i \cos i_1 \quad (59)$$

For the moment ignore the dynamics of the constraint vector, which is in general moving across the sky. Then the only significant dynamics to consider (assuming that the orbit is stable and well behaved) is that of the orbit node: $\Omega = \Omega_o - tC_j \cos i$. We can choose, without loss of generality, $\Omega_o = \Omega_1$, thereby simplifying the expression:

$$\cos P_1 = \sin i \sin i_1 \cos(tC_j \cos i) + \cos i \cos i_1 \quad (60)$$

Note the following inequalities:

$$\cos(i + i_1) \leq \cos P_1 \leq \cos(i - i_1) \quad (61)$$

Then the constraint cone is defined by the condition:

$$i_{C_1} > P_1 \quad (62)$$

or

$$\cos i_{C_1} < \cos P_1 \quad (63)$$

$$\cos i_{C_1} < \sin i \sin i_1 \cos(tC_j \cos i) + \cos i \cos i_1 \quad (64)$$

For this inequality to be satisfied the inclination must lie in the range:

$$i \in [i_1 - i_{C_1}, i_1 + i_{C_1}] \quad (65)$$

If i is not in this interval, then the constraint is never met. Given an inclination within this interval, the constraint may be trivially met by setting $t = 0$. However, as time progresses the inequality may again be violated due to the secular change in the node.

Refering to Inequality 61, we see that if

$$\cos i_{C_1} < \cos(i + i_1) \quad (66)$$

the constraint is never violated and the node can move through a 2π rotation without leaving the constraint cone. Else, if

$$\cos(i + i_1) \leq \cos i_{C_1} \leq \cos(i - i_1) \quad (67)$$

the constraint will be reached at time T:

$$T(i) = \frac{1}{C_j \cos i} \arccos \left[\frac{\cos i_{C_1} - \cos i \cos i_1}{\sin i \sin i_1} \right] \quad (68)$$

Then, performing a maneuver to place the orbit node at $\Omega_1 + C_j \cos iT$, the time until the constraint is violated again is $2T$. Thus, to maximize the time between maneuvers it is necessary to maximize the value of T with respect to inclination i. Note that the coefficient C_j adds nothing to the problem and can be ignored, implying that the optimization is purely geometric and involves no physical quantities

The procedure for the optimization is sketched out below. First, if $0, \pi/2$ or $\pi \in [i_1 - i_{C_1}, i_1 + i_{C_1}]$, then the time optimal inclination is whichever of the three lie in the interval. in all three cases the orbit normal remains fixed in space, and the constraint is satisfied until the constraint vector $\mathbf{u}_1$ moves sufficiently. If neither of these situations occur, then the function $T(i)$ must h e maximized with respect to inclination i. This is a fairly simple procedure and requires the solution of $\partial T/\partial i = 0$. Upon solution, we have the time-optimal inclination i* and the maximum time T^* over the possible values. Thus the orbit plane normal vector which maximizes the time to the next maneuver is specified by the inclination i^* and the node $\Omega^* = \Omega_1 + C_j \cos i^* T^*$, leading to the optimal orbit plane normal:

$$\mathbf{u}_h^* = \sin \Omega^* \sin i^* \hat{x} - \cos \Omega^* \sin i^* y + \cos i^* \hat{z} \tag{69}$$

A further result should also be noted. If the constraint angle $i_{C_1} \geq \pi/4$, then the time-optimal control reduces to a series of inclinations at 0, $\pi/2$ and π. The spacecraft remains at one of these inclinations until the constraint becomes violated due to the motion of $\mathbf{u}_1$. Then a 90° plane change maneuver is performed to the next inclination which satisfies the constraint.

To execute the maneuver, the orbit must be propagated up to the point where its current, or-bit plane intersects with the desired plane, defined above. When at this intersection, a maneuver is performed which rotates the velocity vector by an angle 2 arcsin [sin i sin$(TC_j \cos i)$], with a maneuver magnitude of $\Delta V = 2V \sin i \sin(TC_j \cos i)$, where V is the magnitude of the spacecraft velocity. In actuality, the values of i_1 and Ω_1 vary in time, causing the above analysis to be a bit naive. Note, however, that in this case the above approach is applicable with only slight modification.

5,3.2 Multiple Constraints

The situation is made more difficult when multiple constraint cones exist. The same approach applies in general, although now the checking conditions and time optimization is more difficult. For the NEAR mission there are two cones, which the orbit normal must lie in, called $\mathcal{C}_1$ and $\mathcal{C}_2$ and defined by a unit vector $\mathbf{u}_i$ and constraint angle $i_{C_i} (i = 1, 2)$. "1'best cones correspond to the Earth and Sun respectively. '1'here are three cases to consider here:

$$\mathcal{C}_i \cap \mathcal{C}_j = \emptyset \tag{70}$$

$$\mathcal{C}_i \cap \mathcal{C}_j \in \mathcal{C}_i \tag{71}$$

$$\mathcal{C}_i \cap \mathcal{C}_j \notin \begin{cases} \emptyset \\ \mathcal{C}_i \end{cases} \tag{72}$$

where i and j take on the values 1 or 2 exclusively. Condition 70 means that the constraints are mutually exclusive and cannot be met simultaneously, thus a choice must be made as to which, if either, constraint is to be met. This condition occurs when:

$$\mathbf{u}_1 \cdot \mathbf{u}_2 < \cos(i_{C_1} + i_{C_2}) \tag{73}$$

Condition 71 means that one of the constraint cones lies entirely within the other, and thus the single constraint control as described in the previous subsection can be applied. This condition occurs when:

$$\mathbf{u}_1 \cdot \mathbf{u}_2 > \cos(i_{C_1} - i_{C_2}) \tag{74}$$

Condition 72 means that the constraints intersect) but neither lies completely within the other. The topology of the intersection of these cones describes a variety of potentially different

shapes. It is possible, however, to find the "hounding box" in terms of inclination and node, within whit.11 this area must lie. Simply put:

$$\mathcal{C}_1 \text{ n } \mathcal{C}_2 \in 1 \tag{75}$$

$$\begin{aligned} I = \{&i, \Omega | \\ &i \in [\max(i_1 - i_{C_1}, i_2 - i_{C_2}), \min(i_1 + i_{C_1}, i_2 + i_{C_2})] \\ &\Omega \in [\max(\Omega_1 - \Delta\Omega_1, \Omega_2 - \Delta\Omega_2), \min(\Omega_1 + \Delta\Omega_1, \Omega_2 + \Delta\Omega_2)]\} \end{aligned} \tag{76}$$

$$\Delta\Omega_i = \arccos\left[\frac{\cos i_{C_i} - \cos i \cos i_i}{\sin i \sin i_i}\right] \tag{n}$$

Note that $I \not\subset \mathcal{C}_1 \text{ n } \mathcal{C}_2$ in general, thus the set I may contain angles that are not in the constraint zone. However, these areas tend to be small.

Again, if O, $\pi/2$ or π lie within I (and more specifically within $\mathcal{C}_i \cap \mathcal{C}_j$), then these are once again the time optimal solutions. If not, then it, is necessary to maximize the time which the orbit normal takes to move across the constraint interval in the nodal dimension, where this time T is now computed as:

$$T(i) = \frac{\Delta\Omega}{C_j \cos i} \tag{78}$$

$$\Delta\Omega = \min(\Omega_1 + \Delta\Omega_1, \Omega_2 + \Delta\Omega_2) - \max(\Omega_1 - \Delta\Omega_1, \Omega_2 - \Delta\Omega_2) \tag{79}$$

and where $\Delta\Omega_i$ is defined in Equation 77. In the case of a single constraint the function $T(i)$ *was* a continuous and smooth function of inclination. in the current multiple constraint case the function $T(i)$ is now only continuous and not necessarily smooth with respect to inclination. However, it is still possible to robustly solve this equation for the time optimal inclination i^* and node Ω^* which then define the new orbit plane normal $\mathbf{u}_h^*$.

5.4 **Radius Control**

When orbiting closely to a body such as Eros, the use of osculating Keplerian elements for targeting and orbit description is not well defined in general and use of such elements to design orbits and execute maneuvers could have negative consequences. For an interesting, example of the potential deviation of NEAR orbits from the usual osculating Keplerian elements, see Figure 6 which shows the radius, osculating periapsis and osculating apoapsis of a near-circular, retrograde, equatorial orbit. Among the observations to make: the orbit never goes through apoapsis due to the large secular rates of its argument of peri apsis, the orbit goes through multiple periapsis passages during one revolution, and the osculating elements have large amplitude, high frequency terms. Nonetheless, the orbit in question is extremely stable and has no danger of impact or escape. Similar examples abound. The implication drawn from examples such at these are that the osculating elements arc no longer reliable as predictors of an orbit's future evolut ion, and hence are not necessarily good targeting parameters. Even so, the orbits still retain some characteristic features which can be used to t arget maneuvers.

For targeting from a higher, circular orbit to a specified periapsis radius the following procedure is used. Given an initial state $\mathbf{r}_o, \mathbf{v}_o$ define the propagated spacecraft orbit by $\mathbf{r}(t; \mathbf{r}_o, \mathbf{v}_o), \mathbf{v}(t; \mathbf{r}_o, \mathbf{v}_o)$. Next enforce the restriction $\mathbf{r}_o \mathbf{v}_o$ = O and a desired orbit plane, thus leaving the magnitude of the initial velocity $v_o = |\mathbf{v}_o|$ as the free parameter in the targeting problem. Define the functions $\dot{r}(t, v_o) = \mathbf{r} \cdot \mathbf{v}/|\mathbf{r}|$ and $r(t, v_o) = |\mathbf{r}|$. Now define a Poincaré Map from $\dot{r}(0, v_o)$ = O to $\dot{r}(T, v_o)$ = O, and choose the initial velocity v_o to solve the equation $r(T, v_o) - r_p$ = O where r_p is the desired periapsis radius and T is solved for from the implicit equation $\dot{r}(T, v_o) = 0$. This equation is solved using a Newton iteration algorithm, where the partial of these functions can be expressed via the state transition matrix. This approach diveroces itself from osculating; orbital elements and only relies on the geometry of the problem. The argument of this true periapsis is controlled by timing the initial maneuver epoch.

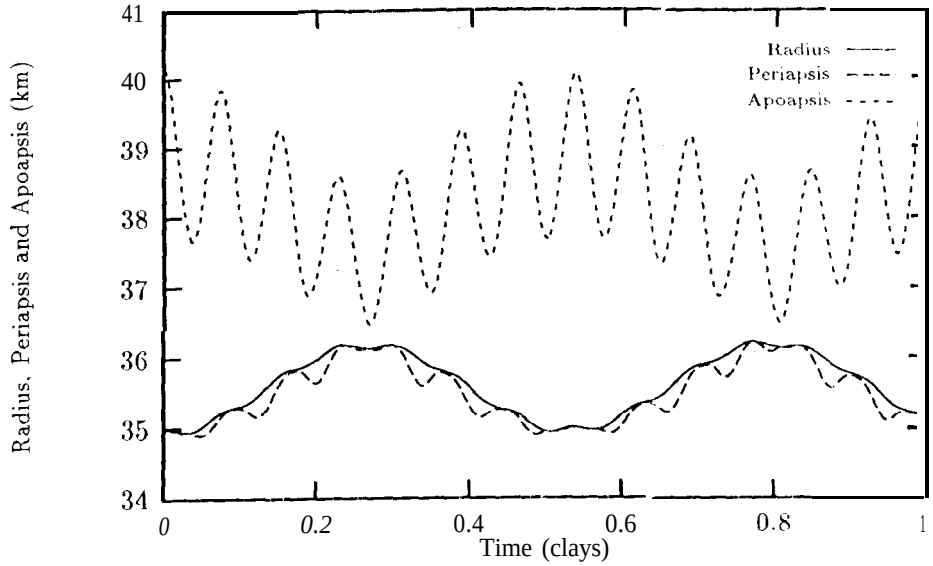

Figure 6: Radius, Apoapsis and Periapsis of a near- circular, retrograde orbit

Once the proper periapsis is targeted and the spacecraft arrives at this radius, it is necessary to design the next maneuver to circularize the orbit. Approaching this task with a traditional appeal to osculating elements again fails to provide a very circular orbit. A better approach is to employ the averaged theory developed for orbiters about oblate bodies (Ref. many), although this still may not yield acceptable results. Through a variety of experiments, it has been found that a robust and simple way to find the proper initial conditions (the velocity) for a circular orbit at a low asteroid altitude is to apply a least-squares approach in targeting the velocity. Given is the initial radius $\mathbf{r}_o$ and desired is to choose the initial velocity $\mathbf{v}_o$, subject to the constraint $\mathbf{r}_o \cdot \mathbf{v}_o = 0$ (and with the desired orbit plane specified), such that the ensuing orbit is as circular as possible. To do so the initial velocity magnitude v_o is chosen to minimize the function:

$$J = \frac{1}{2} \int [r'(t, v_o) - a]^2 \, dt \qquad (80)$$

where a is the circular orbit radius desired. To perform this minimization it is necessary to solve the equation:

$$\frac{\partial J}{\partial v_o} = \int_0^7 [r(t, v_o) - a] \frac{\partial r}{\partial v_0} dt = O \qquad (81)$$

where the partials are evaluated from the state transition matrix. See Figure 7 for a comparision between the radii of three orbits started at a radius of 35 km in a retrograde, equatorial orbit. The initial velocity of these orbits was started normal to the initial radius, and the initial velocity magnitude was chosen by one of the three different methodologies: local circular with no modifications, local circular using modifications from averaged planetary theory, and the minimizing initial velocity from the above scheme.

From Figure 7 it is obvious that the nominal circular velocity is unacceptable for maneuver design as it leads to a ~10% variation in radius (3.5 km) and an effective eccentricity of 0.053. The averaged approach does better, with only a 3.4%0 variation in radius (1.2 km) and an effective eccentricity of 0.017. However, the least-squares approach yields a radius variation of less than 0.35% (0.12 km) and an effective eccentricity of less than 0.003. Thus, the least-squares approach yields a truly near-circular orbit. More importantly, it allows for a greater degree of control over the subsequent or-bit.

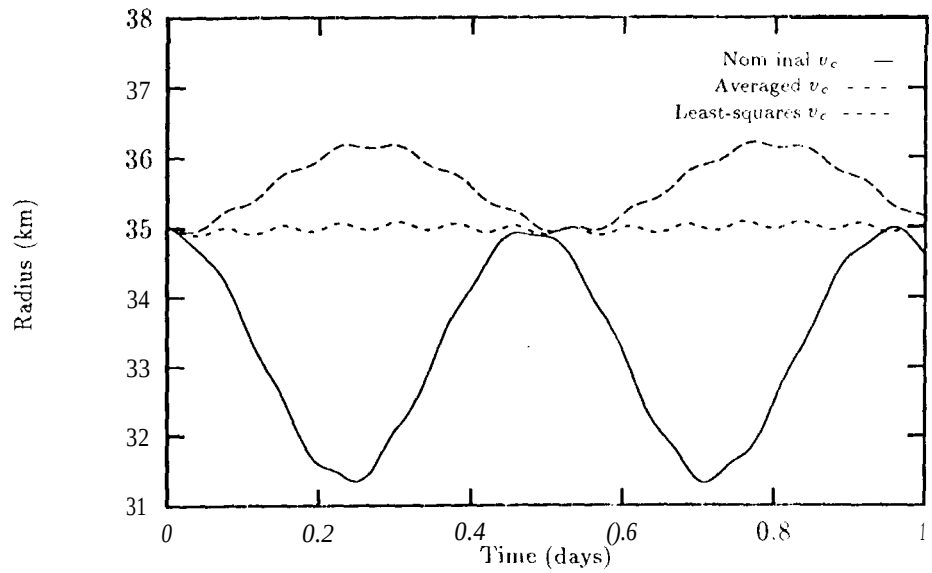

Figure 7: Comparison of initial orbit speed values

With the combination of these two targeting strategies for radial control (along with modifications to them as needed), it is possible to exert a great degree of control over the orbital radius, enabling elliptic orbits will specific, targeted apses and orbits which are as circular as possible. This level of control will be important, as it implies the ability of navigation to deliver orbits to desired geometries and conditions.

5.5 Uncontrolled Elements

Thus far specific mention has been made of controlling four of the six classical elements: a, e, i and Ω. Not considered yet is the control of the the argument of periapsis ω and of the time of periapsis passage of the orbit T_o. Thus far, there have been no specific requirements that the argument of periapsis be controlled during the orbital phase. in far-t, most of the nominal science mapping phase is spent in near circular orbits where the location of the periapsis vector is not a significant consideration. During a few weeks at the beginning of the orbital phase and at the middle of the orbital phase, the spacecraft is nominally in an elliptic 35×50 km orbit. During these times it will be important to carefully target the argument periapsis so that the orbit periapsis lies ahove those regions whose gravity is to be measured. During these orbits, the secular rate of change of the periapsis will be taken to advantage, as it will allow the periapsis to sweep across a range of latitude, providing a more complete survey of the asteroid gravity field.

The final orbital element T_o relates to the timing of the spacecraft in the orbit. Requirements have not been given as of yet on the necessary targeting accuracy needed in this element. Specifically, if it is desired to fly over a particular portion of tile asteroid surface, it is necessary to then control the timing of the spacecraft in the orbit as well as the orbit plane itself. It is usually possible to effect fine control of the orbit timing by adjusting the orbit semi-major axis by small amounts. There arc practical limits within which such adjustments may be made, however. Thus it will be imperative that the orbit timing not be allowed to stray too far from the desired nominal flight path. Should this occur, either *a new* nominal path would be chosen or a pair of larger timing maneuvers would have to be made.

6 Pre-Mission Planning and Plans

Combining the above mission design constraints, navigation needs and scientific concerns, a nominal mission plan has been developed which takes the mission from Eros closest a))pi-each on February 6, 1999 through December 31,]999, the official end date of the mission. Table 1 (Reference[CDR]) summarizes the major events of the nominal mission plan and briefly indicates the rationale behind each phase. Note that the mass and J_2 term used for designing the nominal mission are derived from the values given in REF[Yeomans].

Date	Day	Description	Orbits (km x km)	, inclination (degrees)	Length (days)	Goals
2/ 6/99	0	Eros C/A	Hyperbolic			
2; 8/99	2	Insertion	**1000** × 1000	≈ 147	14	2nd° Gravity
2/22/99	16	Transfer	1000 → 200	≈ 155	7	
3/ 1/99	23	Characterize	*200 x 200*	≈ 162	*10*	4th° Gravity
3/11/99	33	Transfer	*200* + 50	≈ 168	4	
3/15/99	37	Characterize	*50 X50*	17(I	7	Gravity
3/22/99	44	Characterize	*50 x3.5*	170	7	Gravity
3/29/99	51	Characterize	*35 X50*	170	7	Gravity
4/ 5/99	58	Mapping	*35 x 35*	>175 TBD	52	Science Phase
5/27/99	*110*	Mapping	*50* X *50*	*150- 90*	68	Science Phase
8/ 3/99	178	Characterize	50 x 35	90	14	Gravity
8/17/99	192	Mapping	55 x 55	*90*	6	Science Phase
8/23/99	198	Mapping	55 x 55	Plane-flip Maneuver	(-)	Science }'base
8/23/99	198	Mapping	55 x 55	90 –› 167	79	Science Phase
11/10/99	277	Mapping	35 x35	> 145 TBD	*40*	Science Phase
12/20/99	317	Mapping	50 X50	≈ 148	11	Science Phase
12/31/99	328	End of Mission				

"l'able 1: Nominal Mission Timeline

Some of the mission summaries of interest are:

- Total deterministic AV expenditure is 58.2 m/s
- Science days (256 total):

  92 days at the 35 x 35 km equatorial, retrograde orbit

  79 days at the *50* **x 50** krn orbits (inclination from 150- 90°)

  85 days at the 55 x 55 *km* orbits (inclination from 90 →]67°)

  30 days in polar orhit, 14 devoted to navigation gi avity mapping

  Additional sub-solar flyover possible during plane-flip maneuver (around day 198)

- Gravity Mapping periods:

  1 week at 50 x 50 at start of mission

  1 week at 35 x 50 with periapsis 10° above the equator at start of mission

  1 week at 35 x 50 with periapsis 10° below the equator at start of mission

  2 weeks at 35 x 50 polar orbit with periapsis at high latitudes

In implementing the mission design constraints it was found that the 35 × 35 orbits were only feasible when tile Sun and Earth vectors lay close to the rotation pole of 1)ros, and the spacecraft could fly in a near-equatorial orbit without having to perform active maneuvers to control the orhit node. Should the spacecraft perform such maneuvers while at this altitude, the constraint on the

maneuver frequency would be violated; which would in turn impact the operational intensity of the mission during this phase. The dates of these two periods of 35 x 35 orbits are from 4/5/99 through 5/27/99 and from 11/10/99 through 12/20/99. The initial period is shortened somewhat from its potential length due to navigation activities necessary to sup port a transfer to such a low orbit. Au earlier arrival date would alleviate this penalty and add up to 15 days at the low altitude. Should the actual rotation pole at Eros be significantly different from the current nominal value, the mission timeline may be significantly perturbed. Figure 8 shows the Sun and Earth inclination as measured from the rotation pole of Eros. A necessary condition for the spacecraft, to fly at the lower altitude orbits without having to make frequent plane changes is that both the Sun and Earth be witbin their constraint angles i_C or $\pi - i_C$ of the Eros rotation pole.

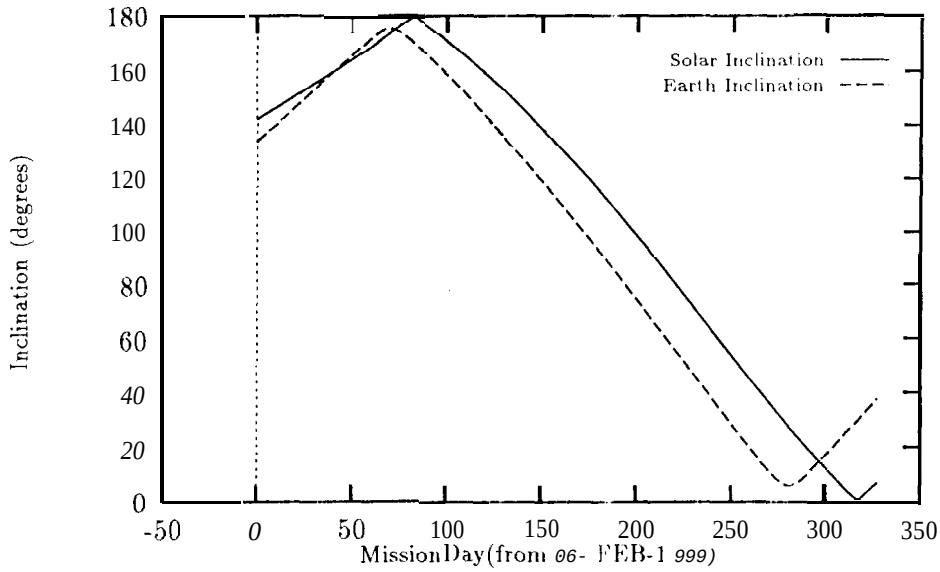

Figure 8: Sun and Earth inclination with respect to Eros' Rotation Pole

There are a variety of science issues and concerns that have not been dealt with to date. These include modifying the orbit inclination during the 35 x 3501 bit phases to allow for different viewing geometries, or considering what possible off-nadir pointing constraints apply to the spacecraft during the mission. While in the 35 x 35 orbit phase, it costs ≈ 9.4 cm/sec for every degree of plane change, yielding ample margin for a variety of plane change maneuvers at this altitude, if desirable. There will still be time constraints on the frequency of such maneuvers, and some assurance must always be present, that the spacecraft, orbit will in fact be stable at the desired itlclirlation/altitude combination.

7 Conclusions

The NEAR mission to the asteroid Eros will provide a challenge to traditional approaches to orbit control and targeting. By flying in such a dynamic environment, opportunities to find new phenomenon and to complement existing understanding of orbital dynamics will abound. Challenges will assert themselves in many forms, from support iug scientific goals to safely controlling and navigating the spacecraft in its orbit.

Acknowledgments

The research described in this paper \vas carried out by the Jet Propulsion Laboratory, California Institute of Technology, under contract with the National Aeronautics and Space Administration.

References

[1] D. Brouwer & G. M. Clemence, Methods of Celestial Mechanics, Academic Press, 1961.

[2] J.M.A. Danby, Fundamentals of Celestial Mechanics, 2nd Ed., Willmann-Bell, 1988.

[3] D.J. Scheeres, "Dynamics about Uniformly Rotating TriAxial Ellipsoids: Applications to Asteroids", Icarus **110,** 225-238, 1994,

[4] D.J. Scheeres, B.G. Williams, W.E. Bollman, R.P. Davis, C.E. Helfrich, S.1'. Synnott, D.K. Yeomans, "Navigation for Low- Cost Missions to Small Solar System Bodies", Acta Astronautic, Vol 35, Suppl., pp 211 -220, 1995

[5] D.J..Scheeres, "Satellite Dynamics About Asteroids", Paper AAS 94- 112, presented at the AA S/AIAA Spaceflight Mechanics Meeting, Cocoa Beach. FL, February 14-16, 1994,

[6] D.K. Yeomans, "433 Eros - Updated Orbit and Physical Characteristics", JPL-IOM 314.10-110 (internal document), January 23, 1995,

[7] D. Brouwer, "Solution of the Problem of Artificial Satellite Theory Without Drag", The Astronomical Journal, 64, 378- 397, 1959 ,

[8] B. Chauvineau, P. Farinella & F. Mignard, "Planar orbits about a Triaxial Body: Application] to Asteroidal Satellites",' Icarus, 105, 370-384, 1993.

[9] Garfinkel, B., 1958. On the Motion of a Satellite of an Oblate Planet, *The Astronomical Journal*, **63**, 88 -96.

[10] German, D., A. Friedlander, 1991. A Simulation of Orbits Around Asteroids Using Potential Field Modeling. *Proc. AAS/AIAA Spaceflight Mechanics Meeting*, Houston, TX, February 11-13, 1991.

[11] Kaula, W.M., 1966. *Theory of Satellite Geodesy*, Blaisdell,

[12] Kozai, Y., 1959. The Motion of a Close Earth Satellite, *The Astronomical Journal*, **64**, *367-377.*,